Analysis of brain atrophy and local gene expression implicates astrocytes in Frontotemporal dementia

Authors:

Andre Altmann PhD[1], David M Cash PhD[1,2], Martina Bocchetta PhD[2], Carolin Heller BSc[2], Regina Reynolds[2], Katrina Moore BSc[2], Rhian S Convery MSc[2], David L Thomas PhD[3], John van Swieten PhD[4], Fermin Moreno MD PhD[5], Raquel Sanchez-Valle PhD[6], Barbara Borroni MD[7], Robert Laforce Jr MD PhD[8], Mario Masellis MD PhD[9], Maria Carmela Tartaglia MD[10], Caroline Graff MD PhD[11], Daniela Galimberti PhD[12,13], James B. Rowe FRCP PhD[14], Elizabeth Finger MD[15], Matthis Synofzik MD[16,17], Rik Vandenberghe MD PhD[18], Alexandre de Mendonça MD PhD[19], Fabrizio Tagliavini MD[20], Isabel Santana MD PhD[21], Simon Ducharme MD[22], Chris Butler FRCP PhD[23], Alex Gerhard FRCP PhD[24], Johannes Levin MD[25,26,27], Adrian Danek MD[25], Giovanni Frisoni PhD[28], Roberta Ghidoni PhD[29], Sandro Sorbi PhD[30], Markus Otto MD[31], Mina Ryten MD PhD[2], Jonathan D Rohrer FRCP PhD[2], on behalf of the Genetic FTD Initiative, GENFI.*

Affiliations:

[1]Centre of Medical Image Computing, Department of Medical Physics, University College London, London, UK

[2]Dementia Research Centre, Department of Neurodegenerative Disease, UCL Queen Square Institute of Neurology, University College London, London, UK

[3]Neuroimaging Analysis Centre, Department of Brain Repair and Rehabilitation, UCL Institute of Neurology, Queen Square, London, UK.

[4]Department of Neurology, Erasmus Medical Centre, Rotterdam, Netherlands

[5]Cognitive Disorders Unit, Department of Neurology, Donostia University Hospital, San Sebastian, Gipuzkoa, Spain.

[6]Alzheimer's disease and Other Cognitive Disorders Unit, Neurology Service, Hospital Clínic, University of Barcelona, Barcelona, Spain.

[7]Centre for Neurodegenerative Disorders, Neurology Unit, Department of Clinical and Experimental Sciences, University of Brescia, Brescia, Italy.

[8]Clinique Interdisciplinaire de Mémoire du CHU de Québec, Département des Sciences Neurologiques Université Laval Québec, Québec, Canada.

[9]Sunnybrook Health Sciences Centre, Sunnybrook Research Institute, University of Toronto, Toronto, Canada.

[10]Tanz Centre for Research in Neurodegenerative Diseases, University of Toronto, Toronto, Canada.

[11]Department of Geriatric Medicine, Karolinska University Hospital-Huddinge, Stockholm, Sweden.

[12]Dept. of Biomedical, Surgical and Dental Sciences, University of Milan, Centro Dino Ferrari, Milan, Italy.

[13]Fondazione IRCCS Ca' Granda, Ospedale Maggiore Policlinico, Milan, Italy.

[14]Department of Clinical Neurosciences, University of Cambridge, Cambridge, United Kingdom.

[15]Department of Clinical Neurological Sciences, University of Western Ontario, London, Ontario Canada.

[16]Department of Neurodegenerative Diseases, Hertie-Institute for Clinical Brain Research and Center of Neurology, University of Tübingen, Tübingen, Germany.

[17]German Center for Neurodegenerative Diseases (DZNE), Tübingen, Germany.

[18]Laboratory for Cognitive Neurology, Department of Neurosciences, KU Leuven, Leuven, Belgium.

[19]Laboratory of Neurosciences, Institute of Molecular Medicine, Faculty of Medicine, University of Lisbon, Lisbon, Portugal.

[20]Fondazione Istituto di Ricovero e Cura a Carattere Scientifico Istituto Neurologica Carlo Besta, Milano, Italy.

[21]Faculty of Medicine, University of Coimbra, Coimbra, Portugal.

[22]Department of Psychiatry, McGill University Health Centre, McGill University, Montreal, Québec, Canada.

[23]Nuffield Department of Clinical Neurosciences, Medical Sciences Division, University of Oxford, Oxford, United Kingdom.

[24]Faculty of Medical and Human Sciences, Institute of Brain, Behaviour and Mental Health, University of Manchester, Manchester, UK.

[25]Department of Neurology, Ludwig-Maximilians-University, Munich, Germany.

[26]German Center for Neurodegenerative Diseases (DZNE), Munich, Germany.

[27]Munich Cluster for Systems Neurology (SyNergy), Munich, Germany.

[28]Instituto di Recovero e Cura a Carattere Scientifico Istituto Centro San Giovanni di Dio Fatebenefratelli, Brescia, Italy.

[29]Molecular Markers Laboratory, IRCCS Istituto Centro San Giovanni di Dio Fatebenefratelli, Brescia, Italy

[30]Department of Neuroscience, Psychology, Drug Research, and Child Health, University of Florence, Florence, Italy.

[31]Department of Neurology, University of Ulm, Ulm.

Short Title: Spatial gene expression and FTD

Corresponding author:

Dr. Andre Altmann

Email: a.altmann@ucl.ac.uk

Words: 3,596

Abstract

Frontotemporal dementia (FTD) is a heterogeneous neurodegenerative disorder characterized by neuronal loss in the frontal and temporal lobes. Despite progress in understanding which genes are associated with the aetiology of FTD (*C9orf72*, *GRN* and *MAPT*), the biological basis of how mutations in these genes lead to cell loss in specific cortical regions remains unclear. In this work we combined gene expression data for 16,912 genes from the Allen Institute for Brain Science atlas with brain maps of gray matter atrophy in symptomatic *C9orf72*, *GRN* and *MAPT* carriers obtained from the Genetic FTD Initiative study. A set of 405 and 250 genes showed significant positive and negative correlation, respectively, with atrophy patterns in all three maps. The gene set with increased expression in spared cortical regions, i.e., signaling regional resilience to atrophy, is enriched for neuronal genes, while the gene set with increased expression in atrophied regions, i.e., signaling regional vulnerability, is enriched for astrocyte genes. Notably, these results extend earlier findings from proteomic analyses in the same cortical regions of interest comparing healthy controls and patients with FTD. Thus, our analysis indicates that cortical regions showing the most severe atrophy in genetic FTD are those with the highest astrocyte density in healthy subjects. Therefore, astrocytes may play a more active role in the onset of neurodegeneration in FTD than previously assumed, e.g., through emergence of neurotoxic (A1) astrocytes.

Keywords:

Frontotemporal dementia, atrophy, gene expression, astrocytes, imaging genetics

Abbreviated summary (50 words):

Altmann et al. investigated the concordance between spatial cortical gene expression in healthy subjects and atrophy patterns in genetic frontotemporal dementia. They found that gene expression of astrocyte-related genes was higher in regions with atrophy. Thus, suggesting a more active role of astrocytes in the onset of neurodegeneration.

Abbreviations

AIBS	Allen Institute for Brain Science
C9orf72	Chromosome 9 open reading frame 72 gene
EWCE	Expression Weighted Cell-type Enrichment
FTD	Frontotemporal dementia
GENFI	Genetic FTD Initiative
GFAP	glial fibrillary acidic protein
GO	Gene Ontology
GRN	Progrenulin gene
LME	Linear Mixed Effects
LSD	Lysosomal Storage Disorder
MAPT	tau gene
MNI	Montreal Neurological Institute and Hospital
NCL	neuronal ceroid lipofuscinosis
OR	Odds Ratio
VBM	Voxel Based Morphometry

Introduction

Frontotemporal dementia (FTD) is a heterogeneous neurodegenerative disorder characterized by neuronal loss in the frontal and temporal lobes, with clinical symptoms including behavioral, language and motor deficits (Seelaar *et al.*, 2011). Around 30% of FTD is familial, most commonly caused by autosomal dominant genetic mutations in one of three genes: progranulin (*GRN*), microtubule-associated protein tau (*MAPT*) or chromosome 9 open reading frame 72 (*C9orf72*) (Rohrer *et al.*, 2009). Despite progress in understanding the pathophysiological basis of genetic FTD, the biological basis of how mutations in these genes leads to cell loss in specific cortical regions and subsequently to specific clinical phenotypes is unclear.

An alternative approach to elucidate the molecular biology of autosomal dominant FTD is to study the gene expression profiles of brain regions which are atrophic in symptomatic mutation carriers. This approach has been enabled by publicly available data from the Allen Institute for Brain Science (AIBS) which features post-mortem high-resolution brain-wide gene expression data from cognitively normal individuals (Hawrylycz *et al.*, 2012). In recent years the AIBS atlas has been successfully integrated with brain maps obtained from case-control studies. For instance, one study investigated the link between gene expression and both regional patterns of atrophy and amyloid deposition, finding a positive correlation of *APP* gene expression and amyloid (Grothe *et al.*, 2018). A transcriptional analysis of cortical regions vulnerable to cortical thinning in the common epilepsies implicated microglia (Altmann *et al.*, 2018). In the broader FTD context, Rittman *et al.* (2016) studied the expression of *MAPT* in the context of Parkinson's disease and progressive supranuclear palsy.

In this work we combine gene expression data from the AIBS atlas with brain maps of gray matter atrophy in symptomatic *C9orf72, GRN* and *MAPT* mutation carriers from the Genetic FTD Initiative (GENFI) compared with non-carriers (Cash *et al.*, 2017). The aim of this study was to investigate the molecular basis of the atrophy pattern in mutation carriers. We firstly investigated the spatial overlap between gray matter atrophy in each of the three genetic groups and the gene expression of the corresponding gene. Secondly, we aimed to identify which genes showed a high spatial correspondence between their expression throughout the brain and the atrophy pattern in each genetic group. We hypothesized that these genes or

groups of genes may implicate molecular processes or brain cell types that explain why these regions are particularly vulnerable in FTD.

Methods

Allen Human Brain Atlas Data

We used the brain-wide microarray gene expression data generated by the Allen Institute for Brain Science (AIBS) (downloaded from http://human.brain-map.org/) (Hawrylycz *et al.*, 2012). The dataset consists of a total of 3,702 microarray samples from six donors (one female). Each sample comprised 58,692 gene probes and provides coordinates in MNI152 space. The gene expression data have been normalized and corrected for batch effects by the Allen Institute ('TECHNICAL WHITE PAPER: MICROARRAY DATA NORMALIZATION', n.d.). We first restricted the set of samples to cortical regions based on the provided slab type ('*cortex*'), retaining only samples with a maximal distance of 2mm to a cortical region of interest (ROI) obtained by a parcellation (Cardoso *et al.*, 2015) of the study template used in Cash et *al.* (2017) leaving 1,654 microarray samples in total. Next, as previously described (Richiardi *et al.*, 2015) we reannotated all microarray probe sequences with gene names using Re-Annotator (Arloth *et al.*, 2015). We excluded probes that sampled more than one gene (N=6,434), were mapped to intergenic regions (N=91) or could not be mapped to any genomic region (N=1,569), leaving 50,598 probes covering 19,980 unique genes. Furthermore, we removed probes that were marked as expressed in less than 300 of the 1,654 cortical samples (N=12,082). Thus, the analysis was carried out using 37,031 microarray probes covering 16,912 distinct genes. Further, since the majority of the samples were obtained from the left hemisphere, and the high correlation between right and left hemisphere gene expression (Hawrylycz *et al.*, 2012), we attributed all right hemisphere samples to the left hemisphere by mirroring the MNI coordinate at the x-axis.

Image data preparation

In order to quantify the amount of atrophy in carriers of FTD mutations, we used results from a voxel-based morphometry (VBM) analysis of the GENFI dataset (Cash *et al.*, 2017). In particular, in this analysis we used the maps showing the voxel-wise t-statistic (t-maps) comparing symptomatic mutation carriers (*MAPT*: N=10; *GRN*: N=12; *C9orf72*: N=25) to non-carriers (N=144) (Figure 1; top). Here, higher t-scores signify more atrophy in the symptomatic group analysis. A mean bias corrected image from all the normalized T1 images in the GENFI study served as a study template. This template was warped into MNI space using the non-rigid registration based on fast free form deformation implemented in

`NiftyReg` (version 10.4.15) (Modat *et al.*, 2010). The obtained transformation was then applied to each of the three t-maps. For each MNI coordinate of the eligible cortical gene expression samples we located the corresponding voxel in the t-map and extracted a 3x3x3 voxel cube of t-values centered on that MNI coordinate, then the t-score corresponding to a gene expression sample was computed as the mean of the non-zero values in the 3x3x3 cube. This was done in order to accommodate uncertainties in registration. This procedure was carried out for each of the three t-maps and resulted in a 1,654 by three matrix, i.e., each gene expression sample was linked to three t-scores from the VBM analysis (one for each FTD gene).

Association analysis

The overall analysis is depicted in Figure 1. We analyzed the association between atrophy and gene expression in a non-parametric fashion. For a given atrophy map and a given probe, we computed the Spearman (or rank) correlation (ρ) between the local t-score and the gene expression level separately for each of the six donors. We computed separate P-values for positive and negative correlation using the `cor.test` function in R with one-sided hypotheses, respectively. Next, we combined the six p-values for positive correlations into a single meta p-value (P^+) using the sum of Z scores method. The process was repeated for the six p-values for negative correlations (P^-). On purpose, we did not use a weighted approach in order to avoid over-emphasizing the impact of donors with more gene expression samples. This procedure was carried out for each for the 37,031 probes and each of the three genetic group atrophy maps. P-values in each of the six resulting lists were corrected for multiple testing using the method by Holm (Holm, 1979). Significantly positively correlated genes (i.e., higher gene expression is linked to higher atrophy) were those where any probe targeting the gene reached a holm-corrected p-value < 0.05 for positive correlations ($P^+_{Holm} < 0.05$); likewise significantly negatively correlated genes (i.e., higher gene expression is linked to lower atrophy) were required to have a holm-corrected p-value < 0.05 for negative correlations ($P^-_{Holm} < 0.05$) for any of the probes targeting that gene. We also created two overlap lists, one containing the overlap of genes in the three positive lists, the other the overlap of genes in all three negative lists. In the following we refer to these two lists as *consensus* lists. The entire analysis was repeated using a linear mixed effects models (`lme4` package in R (Bates *et al.*, 2015)) for testing the association between gene expression and atrophy. In this analysis the local VBM t-score and donor were the fixed effect and the random effect, respectively. Due to high agreement between the results produced by the two

association approaches, results based on the Spearman correlation analysis will be reported, since it is the approach with the least model assumptions.

Overrepresentation analysis

In order to identify cellular pathways or cellular processes and cell type signature genes that may be enriched in the significant gene lists, we conducted an overrepresentation analysis. We obtained the following gene sets and gene ontologies from the MSigDB database version 6.1 (date accessed 11/23/2017): KEGG (N=186 pathways), REACTOME (N=674 pathways) and Gene Ontology (N=5,917 ontologies). We used Fisher's exact test to compute the p-value for overrepresentation of genes in a given set. All tests were carried out using the 16,912 cortex expressed genes as the background set. For each of the six gene lists (i.e., two per FTD gene) we corrected the p-values using the FDR across all 6,777 pathways and ontologies.

In addition to enrichment analysis for GO terms and pathways we used marker gene lists for six brain cell-types obtained from RNA sequencing of purified human cells (Zhang *et al.*, 2016) to determine if the expressed genes implicate a specific class of brain cell types.

Expression Weighted Cell-Type Enrichment

In an additional analysis we sought to identify potential brain cell types that were implicated by all three FTD genes. To this end we conducted Expression Weighted Cell-type Enrichment (EWCE) analysis (Skene and Grant, 2016) on the two consensus lists using a recently published dataset of brain single-cell sequencing data in the mouse brain that identified 265 different cell types (www.mousebrain.org) (Zeisel *et al.*, 2018). From this dataset we removed 76 cell types that were not directly brain related (e.g., cell belonging to enteric nervous system or the spinal cord), leaving 189 different cell-type signatures. Each of the cell types is also attributed with a high-level annotation (astrocytes, ependymal, immune, neurons, oligos, vascular). In brief, from the single cell mouse dataset we used only genes that had a unique human homolog (1-to-1 mapping). Then, we analyzed the two consensus lists separately for high-level cell type enrichment using EWCE with correction for gene length and GC content. P-values are based on 100,000 permutations and enrichment P-values were corrected for multiple testing using the FDR method. We used the available R package for EWCE.

Results

We tested 16,912 genes (from 37,031 microarray probes) for their association with atrophy pattern across the cortex in genetic FTD using two different approaches (Figure 1). The Spearman rank correlation approach showed a high agreement with the LME-based analysis: the Pearson's correlation coefficient between the two sets of -log10 p-values for each FTD gene ranged from 0.925 to 0.959. The numbers of significant probes ($P_{Holm}<0.05$) and genes with their direction for each of the three FTD genes are listed in Table 1. The association results per probe are available as supplementary material (Dataset S1).

C9orf72

The strongest association between *C9orf72* and the atrophy pattern in symptomatic C9orf72 repeat extension carriers was measured with microarray probe A_23_P405873, which showed a negative Spearman correlation $\rho=-0.0973$ ($P_{uncor}=0.00076$; Figure 2).

The most negatively associated gene was *NEFH* (neurofilament heavy; represented by probe CUST_463_PI416408490; $\rho=-0.35$; P=2.53e-56; Figure 2; Dataset S1). Other negatively correlated genes included those encoding synaptic (*SYT2, VAMP1)* and ion channel proteins (*KCNA1, SCN4B*) (Table 2). Top-ranked gene sets based on the significantly negatively correlated genes include genes related to mitochondria (GO_MITOCHONDRIAL_PART; OR=2.73; $P_{FDR}=2.32e-24$) and the respiratory chain (GO_RESPIRATORY_CHAIN; OR=9.78; $P_{FDR}=1.11e-17$; Dataset S2). Notably, KEGG pathways for neurodegenerative disorders were highly enriched (KEGG_PARKINSONS_DISEASE OR=7.03 $P_{FDR}=2.60e-17$; KEGG_HUNTINGTONS_DISEASE OR=4.81 $P_{FDR}=3.69e-15$; KEGG_ALZHEIMERS_DISEASE OR=5.50 $P_{FDR}=4.67e-17$). Among brain cell types, there was a strong enrichment for neuronal genes (OR=2.57; P=2.83e-37; Dataset S3).

Among the most significantly positively correlated genes were ion channel related genes such as *KCNG1* ($\rho=0.31$; P=2.92e-45), *SCN9A* ($\rho=0.32$; P=8.42e-43) and *KCTD4* ($\rho=0.32$; P=1.46e-44). Top-ranked GO terms for positively correlated genes included cell-cell signaling (GO_CELL_CELL_SIGNALLING, OR=2.31, $P_{FDR}=2.43e-10$; Dataset S2). Among brain cell types, there was a strong enrichment for genes associated with mature astrocytes (OR=4.92; P=2.2e-70) as well as neuronal genes (OR=2.05; P=4.43e-20; Dataset S3).

GRN

The strongest association between *GRN* expression and the atrophy pattern in symptomatic GRN mutation carriers was measured with microarray probe A_23_P49708, which showed a positive Spearman correlation ρ=0.0587 (P_{uncor}=0.0013; Figure 2).

Negatively associated genes include those encoding synaptic proteins (*SLC17A*, Table 2). For the negatively correlated genes, none of the tested gene sets showed statistically significant enrichment after multiple testing correction (Dataset S2). However, among brain cell types, there was a strong enrichment for neuronal genes (OR=2.77; P=8.61e-22; Dataset S3).

Positively associated genes included those encoding proteins involved in the immune response (*CD6*, *WFDC1*, *SPON2*). Top-ranked GO terms (Dataset S2) for positively correlated genes are related to tissue development, (GO_TISSUE_DEVELOPMENT OR=2.2 PFDR=2.58e-12), the extracellular matrix (GO_EXTRACELLULAR_MATRIX OR=3.28 PFDR=1.4e-10) and response to wounding (GO_RESPONSE_TO_WOUNDING OR=2.51 PFDR=2.10e-07). Again, genes related to mature astrocytes showed the strongest enrichment (OR=3.34; P=8.23e-28), followed by endothelial cells (OR=2.17; P=2.59e-06) and weak enrichment for neuron related genes (OR=1.28; P=0.0076; Dataset S3).

MAPT

The strongest association between *MAPT* expression and the atrophy pattern in symptomatic MAPT mutation carriers was measured with microarray probe CUST_449_PI416408490, which showed a positive Spearman correlation ρ=0.0831 (P_{uncor}=1.96e-07; Figure 2).

Among the most significantly negatively correlated genes were those encoding ion channels (*SCN1B*, *SCN1A*, *SLC24A2*, Table 2). As in the case of *C9orf72*, the significantly negatively correlated genes showed enrichment for mitochondria (GO_MITOCHONDRIAL_PART; OR=1.69; P_{FDR}=6.06e-09) and cellular respiration (GO_CELLULAR_RESPIRATION; OR=3.11; P_{FDR}=1.07e-07; Dataset S2). Notably, neuron related genes were strongly enriched (OR=1.85; P=1.59e-26) as well as genes associated with neurodegenerative disorders in KEGG (KEGG_PARKINSON OR=3.19 P_{FDR}=1.23e-06; KEGG_ALZHEIMERS_DISEASE OR=2.49 P_{FDR}=1.97e-05; KEGG_HUNTINGTONS_DISEASE OR=2.36 P_{FDR}=3.17e-05).

Significantly positively associated genes included those encoding ion channels (*KCTD4, SCN9A)*. Significantly positively correlated genes are enriched for cell movement (GO_MOVEMENT_OF_CELL_OR_SUBCELLULAR_COMPONENT; OR=1.63, P_{FDR}=4.66e-09) and neuron projection (GO_NEURON_PROJECTION_DEVELOPMENT; OR=1.90; P_{FDR}=5.34e-08). Furthermore, the positively correlated genes were enriched for genes related to mature astrocytes (OR=4.66, P=1.43e-90), microglia (OR=1.88, P=2.63e-16) and for neurons (OR=1.48, P=1.66e-10; Dataset S3).

Cell-type analysis

From the gene lists obtained for each of the FTD gene atrophy maps we created two consensus lists: one comprising 405 genes that were significantly positively correlated with atrophy in all three FTD genes and one list comprising the 250 genes that were significantly negatively correlated in all three maps (Figure 1). Using these lists, we aimed to identify a common theme underlying the atrophy in the three causative genes. In particular, we used EWCE paired with high resolution cell specific murine gene expression profiles to identify specific cell-types that are enriched in genes that showed significant correlations with atrophy in all three FTD maps. EWCE was executed twice, once using 189 cell-type annotations and once using high-level annotations. The high-level analysis EWCE showed a strong enrichment for astrocyte marker genes (Figure 3; Z-score=5.75; P<0.00001) and a borderline enrichment for ependymal marker genes (Z-score=2.76; P=0.004) among genes with positive correlation to atrophy severity. Genes negatively correlated with atrophy were enriched for neuronal marker genes (Z-score=6.58; P<0.00001). These results were confirmed using cell-type marker genes derived from RNA sequencing of purified human cells (Zhang *et al.*, 2016) (Figure 3; right column).

Discussion

We investigated the gene expression correlates of the cortical regions specifically atrophic in the three main genetic causes of FTD (*MAPT*, *C9orf72*, *GRN*). Overall, the analysis showed that the most atrophic cortical regions in symptomatic mutation carriers have a markedly different gene expression profile in the six cognitively normal subjects from the AIBS gene expression dataset. The type of gene expression profiling used in AIBS is based on measuring

bulk expression of tissue samples, i.e., a group of diverse cell types is sampled at once and the resulting expression profile represents the group average of this set of cells and their states. Thus, in this type of analysis, genes positively correlated with atrophy indicate potential cellular processes and cell types that promote atrophy in genetic FTD. Conversely, genes that are negatively correlated with atrophy indicate potential cellular processes and cell types that confer resilience to disease-related neurodegeneration. Whilst there is no association with expression of the gene itself (i.e., *GRN, MAPT* and *C9orf72*) in each form of genetic FTD, our analysis revealed that groups of genes commonly associated with astrocytes showed higher expression levels in regions with more atrophy and genes commonly associated with neurons showed higher expression levels in the relatively spared regions.

Astrocytes are the most abundant cell-type in the human CNS and they carry out a plethora of functions including biochemical support for the blood-brain barrier-forming endothelial cells, trophic support for neurons, regulation of extracellular ion balance and participation in repair and scarring processes of the brain following injuries. Astrocytes reacting to injuries in the central nervous system, reactive astrocytes, are characterized by expression of glial fibrillary acidic protein (GFAP). Depending on the context, such reactive $GFAP^+$-astrocytes can be neurotoxic (Liddelow and Barres, 2015; Liddelow *et al.*, 2017) or neuroprotective (Anderson *et al.*, 2016). There are already multiple lines of evidence linking astrocyte (dys-)function to neurodegeneration (Rodríguez *et al.*, 2009; Phatnani and Maniatis, 2015; Sofroniew, 2015) and to FTD in particular. For instance, histopathological studies in FTD have shown that severity of astrocytosis and astrocytic apoptosis correlated with the degree of neuronal loss as well as with the stage of the disease, while at the same time neuronal apoptosis was rare (Broe *et al.*, 2004). In addition, astrocyte reactivity appears to be region specific in that higher numbers of reactive ($GFAP^+$) astrocytes were found in the frontal and temporal cortices of FTD patients compared to controls (Martinac *et al.*, 2001). These observations extend to the CSF where levels of GFAP were increased in various neurodegenerative disorders compared to cognitively normal adults with the highest levels in FTD patients (Ishiki *et al.*, 2016). Martinac et *al.* (2001) found that degrading astrocytes were inversely correlated with cerebral blood flow in FTD. However, more importantly, astrocytes derived from induced pluripotent stem cells of patients with mutations in *MAPT* were found to demonstrate increased vulnerability to oxidative stress and exhibit disease-associated gene-expression changes (Hallmann *et al.*, 2017). Co-culture experiments of such modified FTD

astrocytes with previously healthy neurons led, among other things, to increased oxidative stress in these neurons.

Hence, taken together astrocyte reactivity and activation of GFAP co-occur with disease onset and disease progression in FTD, but could astrocytes dysfunction alone be the initiator for neurodegeneration in FTD? The answer may lie partially in the lysosomes of astrocytes: studies have demonstrated that neuronal cell-derived proteins such as α-synuclein can be transferred to close-by astrocytes via endocytosis and that these proteins are destined for degradation in the astrocytes' lysosome (Lee *et al.*, 2010). Likewise, astrocytes are known to bind and degrade extracellular amyloid-β, a key player in Alzheimer's disease (Wyss-Coray *et al.*, 2003; Koistinaho *et al.*, 2004). Recent work established a strong link of both Parkinson's disease and FTD with lysosomal storage disorders (LSDs) (Deng *et al.*, 2015; Burbulla *et al.*, 2017; Evers *et al.*, 2017). LSDs are a large group of rare inherited metabolic disorders with defective lysosome function resulting in faulty degradation and recycling of cellular constituents. Intriguingly, mutations in the familial Parkinson's disease gene *GBA* and the familial FTD gene *GRN* cause the LSDs Gaucher Disease and neuronal ceroid lipofuscinosis (NCL), respectively (Ward *et al.*, 2017). Mounting evidence suggests that astrocyte dysfunction alone is sufficient to trigger neurodegeneration in LSDs (Rama Rao and Kielian, 2016). For instance, in a mouse model astrocyte-specific deletion of *Sumf1* in vivo induced severe lysosomal storage dysfunction in these astrocytes, which in turn was sufficient to induce degeneration of cortical neurons in vivo (Di Malta *et al.*, 2012). More importantly, though, one of the three FTD genes, *GRN*, is also known to cause NCL (Ward *et al.*, 2017) and recent work posits that lysosomal dysfunction is a central disease process in *GRN*-associated FTD (Ward *et al.*, 2017). Indeed, *GRN* is increasingly associated with regulating the formation and function of the lysosome (Kao *et al.*, 2017). In addition, the transcription of *GRN* is co-regulated with other lysosomal genes (Belcastro *et al.*, 2011).

In addition to detecting higher levels of astrocyte-related genes in regions with neurodegeneration in FTD, we found that genes associated with neurons are more enriched in brain regions that are spared in FTD. Moreover, for the *MAPT* and *C9orf72* atrophy maps we additionally noted enrichment for genes that are associated with mitochondria, particularly cellular respiration, in regions that are not affected by atrophy. These results confirm earlier results from an unbiased proteomic screen of tissue samples where the modules related to synapse (M1), mitochondrion (M3) and neuron differentiation (M8) showed negative

correlations with clinicopathological traits in FTD, i.e., these three modules were consistently negatively correlated with FTD pathology (Umoh *et al.*, 2018). Consistent with our results, there was a positive correlation of astrocyte specific modules (M5: Extracellular matrix and M6: Response to biotic stimulus) with clinicopathological traits. While Umoh *et al.* (2018) interpreted the negative (and positive) correlations in part with a disease-related shift in cell population in the sampled ROIs, our results extend this observation to regional cell type densities since the gene expression samples were obtained from six cognitively normal subjects.

Lastly, in the *GRN* group only, there was a positive correlation with a number of genes involved in the immune response (*CD6, WFDC1, SPON2*), i.e., these were associated with the *GRN*-associated FTD pattern of atrophy. This is consistent with previous work showing that inflammation and microglial activation have an aetiological role in *GRN*-associated FTD (Bossù *et al.*, 2011; Martens *et al.*, 2012).

In summary, our analysis indicates that cortical regions showing the most severe atrophy in genetic FTD are those with the highest astrocyte density in healthy subjects. Therefore, astrocytes may have a more active role in the onset of neurodegeneration in FTD than previously assumed. This fits with recent findings of neurotoxic potential of astrocytes (Liddelow *et al.*, 2017). We hypothesize that the distinct regional atrophy pattern in genetic FTD may be driven by regions with naturally increased astrocyte density where these universal astrocyte neurotoxic effects come to bear with higher frequency. Thus, neurodegeneration may be the result of the toxic combination of increased potential for lysosomal storage in astrocytes caused by FTD mutations and age-related increase in neurotoxic (A1) and senescent astrocytes, which lost many normal astrocytic functions.

Funding

AA holds a Medical Research Council eMedLab Medical Bioinformatics Career Development Fellowship. This work was supported by the Medical Research Council (grant number MR/L016311/1). The Dementia Research Centre is supported by Alzheimer's Research UK, Brain Research Trust, and The Wolfson Foundation. This work was supported by the NIHR Queen Square Dementia Biomedical Research Unit, the NIHR UCL/H Biomedical Research Centre and the Leonard Wolfson Experimental Neurology Centre (LWENC) Clinical Research Facility as well as an Alzheimer's Society grant (AS-PG-16-007). JDR is supported by an Medical Research Council Clinician Scientist Fellowship (MR/M008525/1) and has received funding from the NIHR Rare Disease Translational Research Collaboration (BRC149/NS/MH). This work was also supported by the Medical Research Council UK GENFI grant (MR/M023664/1). M.R. holds an Medical Research Council Clinician Scientist Fellowship (grant number MR/N008324/1). R.H.R. was supported through the award of a Leonard Wolfson Doctoral Training Fellowship in Neurodegeneration. This work was supported by Italian Ministry of Health (CoEN015 and Ricerca Corrente). Several authors of this publication (JvS, MS, RV, AD, MO, JR) are members of the European Reference Network for Rare Neurological Diseases - Project ID No 739510. This project was supported, in part, via the European Union’s Horizon 2020 research and innovation program grant 779257 “Solve-RD” (to M.S.).

References

Altmann A, Ryten M, Nunzio M Di, Ravizza T, Tolomeo D, Reynolds RH, et al. A systems-level analysis highlights microglial activation as a modifying factor in common forms of human epilepsy. bioRxiv 2018: https://doi.org/10.1101/470518.

Anderson MA, Burda JE, Ren Y, Ao Y, O'Shea TM, Kawaguchi R, et al. Astrocyte scar formation aids central nervous system axon regeneration. Nature 2016; 532: 195–200.

Arloth J, Bader DM, Röh S, Altmann A. Re-Annotator: Annotation Pipeline for Microarray Probe Sequences. PLoS One 2015; 10: e0139516.

Bates D, Mächler M, Bolker B, Walker S. Fitting linear mixed-effects models using lme4. J Stat Softw 2015

Belcastro V, Siciliano V, Gregoretti F, Mithbaokar P, Dharmalingam G, Berlingieri S, et al. Transcriptional gene network inference from a massive dataset elucidates transcriptome organization and gene function. Nucleic Acids Res 2011; 39: 8677–88.

Bossù P, Salani F, Alberici A, Archetti S, Bellelli G, Galimberti D, et al. Loss of function mutations in the progranulin gene are related to pro-inflammatory cytokine dysregulation in frontotemporal lobar degeneration patients. J Neuroinflammation 2011; 8: 65.

Broe M, Kril J, Halliday GM. Astrocytic degeneration relates to the severity of disease in frontotemporal dementia. Brain 2004; 127: 2214–2220.

Burbulla LF, Song P, Mazzulli JR, Zampese E, Wong YC, Jeon S, et al. Dopamine oxidation mediates mitochondrial and lysosomal dysfunction in Parkinson's disease. Science (80-) 2017; 357: 1255–1261.

Cardoso MJ, Modat M, Wolz R, Melbourne A, Cash D, Rueckert D, et al. Geodesic Information Flows: Spatially-Variant Graphs and Their Application to Segmentation and Fusion. IEEE Trans Med Imaging 2015; 34: 1976–1988.

Cash DM, Bocchetta M, Thomas DL, Dick KM, van Swieten JC, Borroni B, et al. Patterns of gray matter atrophy in genetic frontotemporal dementia: results from the GENFI study. Neurobiol Aging 2017; 62: 191–196.

Deng H, Xiu X, Jankovic J. Genetic Convergence of Parkinson's Disease and Lysosomal Storage Disorders. Mol Neurobiol 2015; 51: 1554–68.

Evers BM, Rodriguez-Navas C, Tesla RJ, Prange-Kiel J, Wasser CR, Yoo KS, et al. Lipidomic and Transcriptomic Basis of Lysosomal Dysfunction in Progranulin Deficiency. Cell Rep 2017; 20: 2565–2574.

Grothe MJ, Sepulcre J, Gonzalez-Escamilla G, Jelistratova I, Schöll M, Hansson O, et al. Molecular properties underlying regional vulnerability to Alzheimer's disease pathology. Brain 2018; 141: 2755–2771.

Hallmann A-L, Araúzo-Bravo MJ, Mavrommatis L, Ehrlich M, Röpke A, Brockhaus J, et al. Astrocyte pathology in a human neural stem cell model of frontotemporal dementia caused by mutant TAU protein. Sci Rep 2017; 7: 42991.

Hawrylycz MJ, Lein ES, Guillozet-Bongaarts AL, Shen EH, Ng L, Miller JA, et al. An anatomically comprehensive atlas of the adult human brain transcriptome. Nature 2012; 489: 391–399.

Holm S. A simple sequentially rejective multiple test procedure. Scand J Stat 1979; 6: 65–70.

Ishiki A, Kamada M, Kawamura Y, Terao C, Shimoda F, Tomita N, et al. Glial fibrillar acidic protein in the cerebrospinal fluid of Alzheimer's disease, dementia with Lewy bodies, and frontotemporal lobar degeneration. J Neurochem 2016; 126: 258–61.

Kao AW, McKay A, Singh PP, Brunet A, Huang EJ. Progranulin, lysosomal regulation and neurodegenerative disease. Nat Rev Neurosci 2017; 18: 325–333.

Koistinaho M, Lin S, Wu X, Esterman M, Koger D, Hanson J, et al. Apolipoprotein E promotes astrocyte colocalization and degradation of deposited amyloid-β peptides. Nat Med 2004; 10: 719–26.

Lee HJ, Suk JE, Patrick C, Bae EJ, Cho JH, Rho S, et al. Direct transfer of α-synuclein from neuron to astroglia causes inflammatory responses in synucleinopathies. J Biol Chem 2010; 285: 9262–72.

Liddelow S, Barres B. SnapShot: Astrocytes in Health and Disease. Cell 2015; 162: 1170.

Liddelow SA, Guttenplan KA, Clarke LE, Bennett FC, Bohlen CJ, Schirmer L, et al. Neurotoxic reactive astrocytes are induced by activated microglia. Nature 2017; 541: 481–487.

Di Malta C, Fryer JD, Settembre C, Ballabio A. Astrocyte dysfunction triggers neurodegeneration in a lysosomal storage disorder. Proc Natl Acad Sci U S A 2012; 109: e2334-42.

Martens LH, Zhang J, Barmada SJ, Zhou P, Kamiya S, Sun B, et al. Progranulin deficiency promotes neuroinflammation and neuron loss following toxin-induced injury. J Clin Invest 2012; 122: 3955–9.

Martinac JA, Craft DK, Su JH, Kim RC, Cotman CW. Astrocytes degenerate in frontotemporal dementia: Possible relation to hypoperfusion. Neurobiol Aging 2001; 22: 195–207.

Modat M, Ridgway GR, Taylor ZA, Lehmann M, Barnes J, Hawkes DJ, et al. Fast free-form deformation using graphics processing units. Comput Methods Programs Biomed 2010; 98: 278–284.

Phatnani H, Maniatis T. Astrocytes in neurodegenerative disease. Cold Spring Harb Perspect Biol 2015; 7: a020628.

Rama Rao K V., Kielian T. Astrocytes and lysosomal storage diseases. Neuroscience 2016; 323: 195–

206.

Richiardi J, Altmann A, Milazzo A-C, Chang C, Chakravarty MM, Banaschewski T, et al. Correlated gene expression supports synchronous activity in brain networks. Sci (New York, NY) 2015; 348: 1241–1244.

Rittman T, Rubinov M, Vértes PE, Patel AX, Ginestet CE, Ghosh BCP, et al. Regional expression of the MAPT gene is associated with loss of hubs in brain networks and cognitive impairment in Parkinson disease and progressive supranuclear palsy. Neurobiol Aging 2016; 48: 153–160.

Rodríguez JJ, Olabarria M, Chvatal A, Verkhratsky A. Astroglia in dementia and Alzheimer's disease. Cell Death Differ 2009; 16: 378–385.

Rohrer JD, Guerreiro R, Vandrovcova J, Uphill J, Reiman D, Beck J, et al. The heritability and genetics of frontotemporal lobar degeneration. Neurology 2009; 73: 1451–1465.

Seelaar H, Rohrer JD, Pijnenburg YAL, Fox NC, Van Swieten JC. Clinical, genetic and pathological heterogeneity of frontotemporal dementia: A review. J Neurol Neurosurg Psychiatry 2011; 82: 476–86.

Skene NG, Grant SGN. Identification of vulnerable cell types in major brain disorders using single cell transcriptomes and expression weighted cell type enrichment. Front Neurosci 2016; 10: 16.

Sofroniew M V. Astrocyte barriers to neurotoxic inflammation. Nat Rev Neurosci 2015; 16: 249–263.

Umoh ME, Dammer EB, Dai J, Duong DM, Lah JJ, Levey AI, et al. A proteomic network approach across the ALS - FTD disease spectrum resolves clinical phenotypes and genetic vulnerability in human brain. EMBO Mol Med 2018; 10: 48–62.

Ward ME, Chen R, Huang HY, Ludwig C, Telpoukhovskaia M, Taubes A, et al. Individuals with progranulin haploinsufficiency exhibit features of neuronal ceroid lipofuscinosis. Sci Transl Med 2017; 9: eaah5642.

Wyss-Coray T, Loike JD, Brionne TC, Lu E, Anankov R, Yan F, et al. Adult mouse astrocytes degrade amyloid-β in vitro and in situ. Nat Med 2003; 9: 453–7.

Zeisel A, Hochgerner H, Lönnerberg P, Johnsson A, Memic F, van der Zwan J, et al. Molecular Architecture of the Mouse Nervous System. Cell 2018; 174: 999-1014.e22.

Zhang Y, Sloan SA, Clarke LE, Caneda C, Plaza CA, Blumenthal PD, et al. Purification and Characterization of Progenitor and Mature Human Astrocytes Reveals Transcriptional and Functional Differences with Mouse. Neuron 2016; 89: 37.

TECHNICAL WHITE PAPER: MICROARRAY DATA NORMALIZATION [Internet]. [cited 2018 Jul 15] Available from: http://help.brain-

map.org/download/attachments/2818165/Normalization_WhitePaper.pdf?version=1&modificationDate=1361836502191&api=v2

Figures

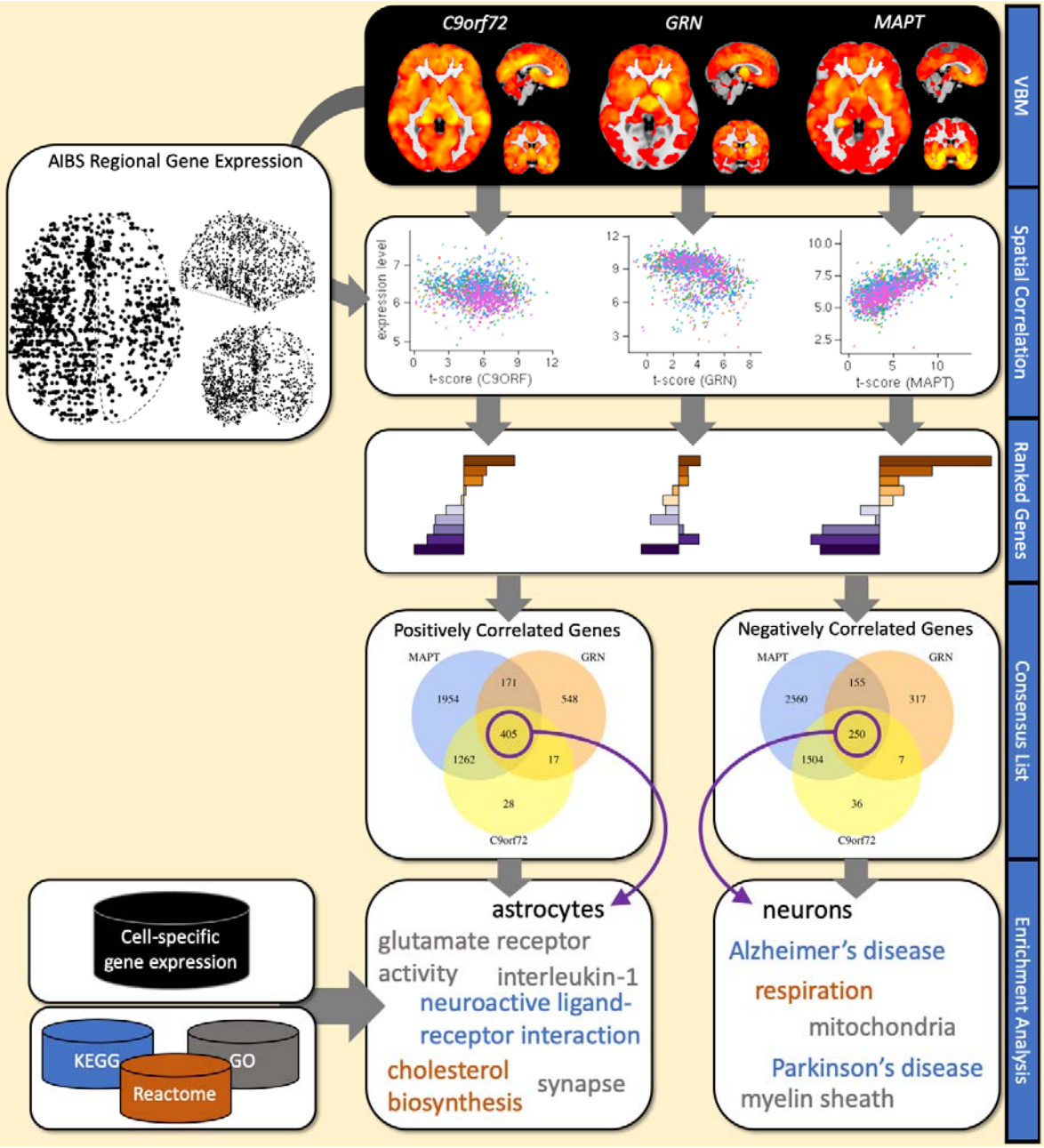

Figure 1: ***Analysis overview.*** Starting point of the analysis are the statistical maps from voxel-based morphometry analyses (VBM) comparing healthy controls and symptomatic FTD mutation carriers in C9orf72, GRN and MAPT from Cash et *al.* (2017). For each statistical map the spatial correlation with the expression levels 16,912 genes (represented by 37,031 gene expression probes) is computed using data from the Allen Institute for Brain Science (AIBS) gene expression atlas. The resulting gene ranking provides lists of genes that are either significantly ($P_{Holm}<0.05$) positively or negatively correlated with the atrophy

pattern. Two consensus lists are generated from the three lists of positively correlated and negatively correlated genes, respectively. Resulting gene lists are analyzed for enrichment of signature genes for brain cell types, such as neurons, microglia or astrocytes, and biological pathways.

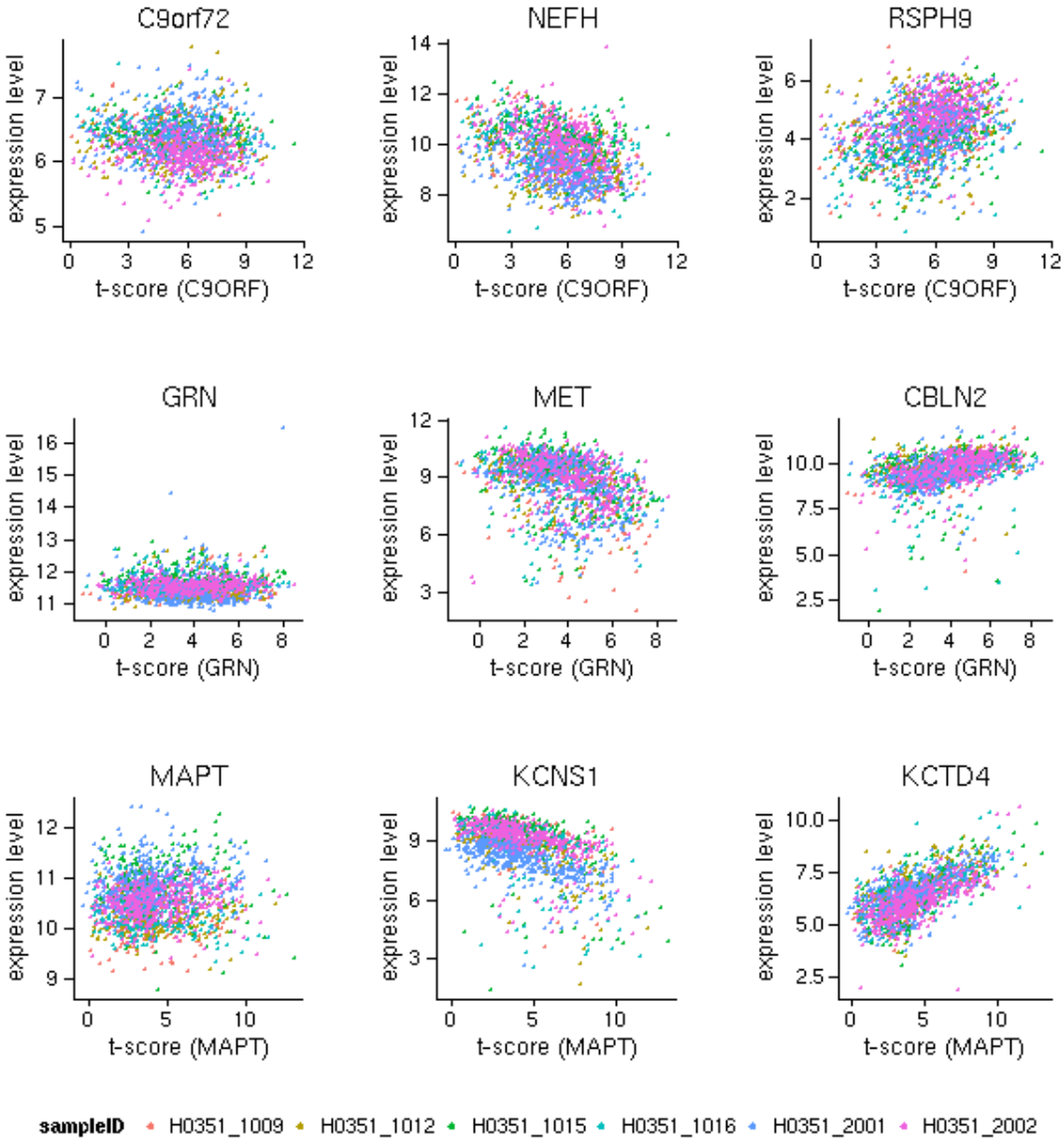

Figure 2: ***Selected scatterplots between t-scores and gene expression levels.*** Rows correspond to the three different FTD genes (*C9orf72*, *GRN* and *MAPT*). X-axes show to the t-value in the corresponding statistical VBM maps (Figure 1) from Cash *et al.* (2017) at positions where microarray samples were obtained in the AIBS atlas; the y-axes represent the expression levels in the AIBS atlas for the gene named at the top of the scatter plot. Each point represents one microarray sample and the color indicates the donor ID. In the first column expression of the corresponding FTD genes is studied: *C9orf72* (A_23_P405873), *GRN* (A_23_P49708) and *MAPT* (CUST_449_PI416408490). The second column shows the most strongly negatively correlated genes, i.e., genes with high expression in brain regions

showing little atrophy: *NEFH* (CUST_463_PI416408490), *MET* (A_23_P359245) and *KCNS1* (A_23_P321846). The third column shows the genes where expression level and atrophy positively correlate the strongest: *RSPH9* (CUST_12355_PI416261804), *CBLN2* (A_23_P15889), *KCTD4* (A_23_P48325).

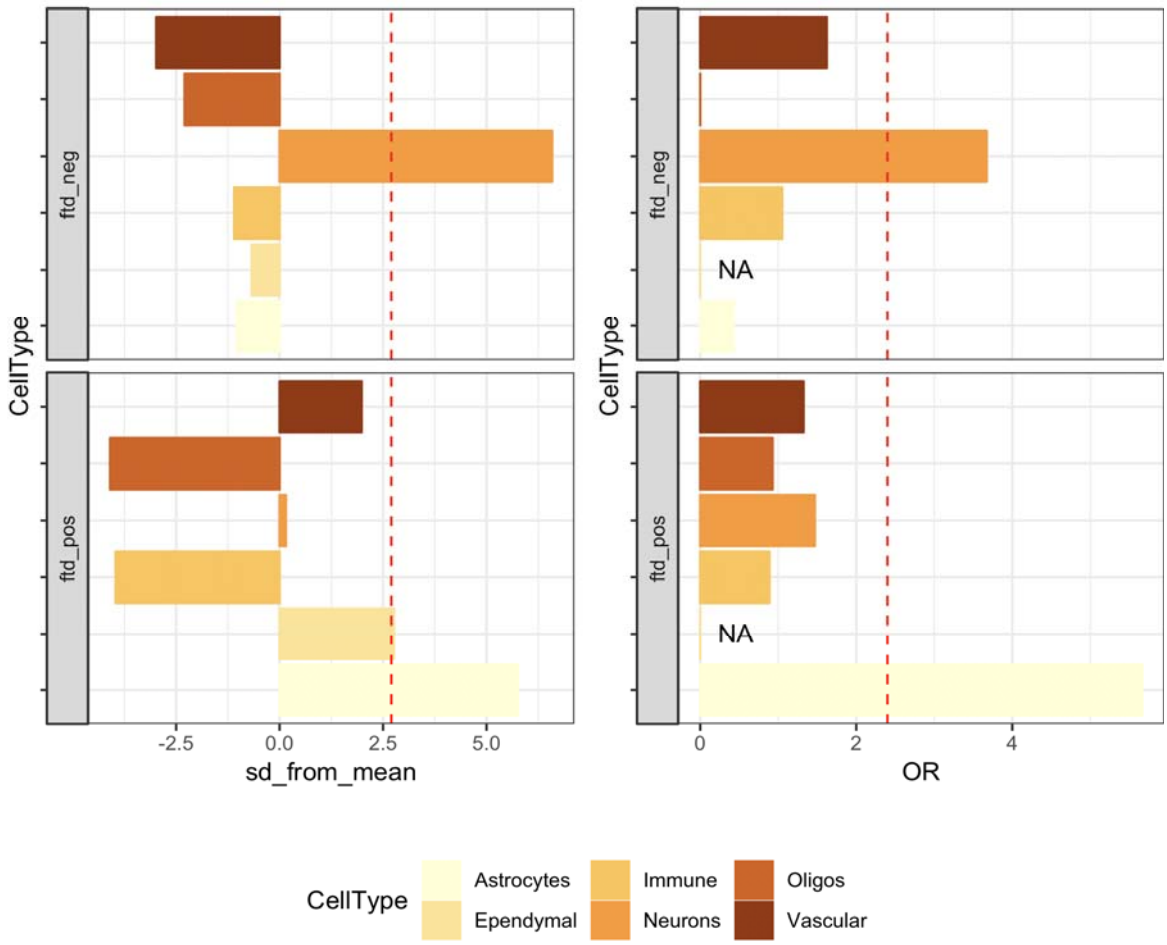

Figure 3: ***Cell-type enrichment in consensus gene lists.*** Two different methods are used to investigate cell type signatures in the two consensus lists. The left panels use the Expression Weighted Cell-type Enrichment (EWCE) method together with single-cell RNA sequencing data from mouse brains (Zeisel *et al.*, 2018); the enrichment is provided as a z-score (i.e., standard deviations (SD) from the mean). The right panels use a classic over-representation analysis based on Fisher's exact test with cell-type signature genes obtained from bulk RNA sequencing of purified human cells (Zhang *et al.*, 2016). Both approaches demonstrate a strong neuronal signal in negatively correlated genes (upper panels) and a strong astrocyte signature in positively correlated genes (lower panels).

Tables

Table 1: Numbers of significant probes and genes and their direction of association after holm correction. Rows correspond to the three genes and an overlap between all three lists.

	Probes		**Genes**	
	positive	**negative**	**positive**	**negative**
C9orf72	2,708	2,861	1,712	1,797
GRN	1,740	1,081	1,141	729
MAPT	6,210	7,528	3,792	4,469
Overlap	607	310	405	250

Table 2: ***Top ten most positively and negatively correlated genes with atrophy patterns in genetic FTD.***

Rank	***C9orf72***		***GRN***		***MAPT***	
	Negative	Positive	Negative	Positive	Negative	Positive
1	*NEFH*	*RSPH9*	*MET*	*CBLN2*	*KCNS1*	*KCTD4*
2	*EPN3*	*ANKRD6*	*KIAA1875*	*GAL*	*NEFH*	*IL13RA2*
3	*SV2C*	*LPPR4*	*SLC17A6*	*ASB2*	*HAPLN4*	*CPNE6*
4	*SYT2*	*KCNG1*	*LXN*	*RTP1*	*EPN3*	*LPPR4*
5	*KCNA1*	*KCTD4*	*ARL9*	*RPH3AL*	*RAB37*	*RSPH9*
6	*KCNS1*	*BAIAP3*	*CPLX2*	*CD6*	*SCN1B*	*ZCCHC12*
7	*ARHGAP9*	*CPNE6*	*TMEM249*	*CTXN3*	*SCN1A*	*LY6H*
8	*PVALB*	*SCN9A*	*MBP*	*PRRX1*	*ESRRG*	*PNMT*
9	*VAMP1*	*TENM3*	*BCL11A*	*TGFBI*	*EIF5A2*	*KCNG1*
10	*CCDC64B*	*PNMT*	*TENM2*	*WFDC1*	*PVALB*	*NECAB2*

Supplementary information

Dataset S1: ***Results from the spatial correlation analysis.*** This table shows for every eligible probe, the mapped gene name, the Spearman (or rank) correlation with the three separate t-maps, P^+ values for positive correlation and P^- values for negative correlation.

Dataset S2: ***Enrichments for pathways.*** Each sheet in this table shows the results of the enrichment analysis for the six gene lists (genes positively and negatively correlated with atrophy, respectively). Columns represent the pathway name, the number of overlapping genes between list and pathway, the expected number of overlapping genes, the odds ratio (OR) and the overrepresentation p-value (including FDR-correction).

Dataset S3: ***Enrichments for brain six cell-types.*** Enrichment analysis testing gene lists with significant positive or negative correlation for cell-type marker genes. Human cell-type gene lists for neurons (N), microglia (MG), mature astrocytes (MA), endothelial cells (EC), oligodendrocytes (OLG) and oligodendrocyte precursor cells (OPC) were obtained from Zhang et al. (2016).

Appendix:

List of GENFI consortium authors:

Caroline Greaves BSc[1], Georgia Peakman MSc[1], Rachelle Shafei MRCP[1], Emily Todd Mres[1], Martin N. Rossor MD FRCP[1], Jason D. Warren PhD FRACP[1], Nick C. Fox MD FRCP[1,2], Henrik Zetterberg[2], Rita Guerreiro PhD[3], Jose Bras PhD[3], Jennifer Nicholas PhD[4], Simon Mead PhD[5], Lize Jiskoot PhD[6], Lieke Meeter MD[6], Jessica Panman MSc[6], Janne Papma PhD[6], Rick van Minkelen PhD[7], Yolanda Pijnenburg PhD[8], Myriam Barandiaran PhD[9,10], Begoña Indakoetxea MD[9,10], Alazne Gabilondo MD[10], Mikel Tainta MD[10], Maria de Arriba BSc[10], Ana Gorostidi PhD[10], Miren Zulaica BSc[10], Jorge Villanua MD PhD[11] Zigor Diaz[12], Sergi Borrego-Ecija MD[13], Jaume Olives MSc[13], Albert Lladó PhD[13], Mircea Balasa PhD[13], Anna Antonell PhD[13], Nuria Bargallo PhD[14], Enrico Premi MD[15], Maura Cosseddu MPsych[15], Stefano Gazzina MD[15], Alessandro Padovani MD PhD[15], Roberto Gasparotti MD[16], Silvana Archetti MBiolSci[17], Sandra Black MD[19], Sara Mitchell MD[19], Ekaterina Rogaeva PhD[20], Morris Freedman MD[21], Ron Keren MD[22], David Tang-Wai MD[23], Linn Öijerstedt MD[24], Christin Andersson PhD[25], Vesna Jelic MD[26], Hakan Thonberg MD[27], Andrea Arighi MD[28,29], Chiara Fenoglio PhD[28,29], Elio Scarpini MD[28,29], Giorgio Fumagalli MD[28,29,30], Thomas Cope MRCP[31], Carolyn Timberlake BSc[31], Timothy Rittman MRCP[31], Christen Shoesmith MD[32], Robart Bartha PhD[33,34], Rosa Rademakers PhD[35], Carlo Wilke MD[36,37], Hans-Otto Karnarth MD[38], Benjamin Bender MD[39], Rose Bruffaerts MD PhD[40], Philip Vandamme MD PhD[41], Mathieu Vandenbulcke MD PhD[42,43], Catarina B. Ferreira MSc[44], Gabriel Miltenberger PhD[45], Carolina Maruta MPsych PhD[46], Ana Verdelho MD PhD[47], Sónia Afonso BSc[48], Ricardo Taipa MD PhD[49], Paola Caroppo MD PhD[50], Giuseppe Di Fede MD PhD[50], Giorgio Giaccone MD[50], Sara Prioni PsyD[50], Veronica Redaelli MD[50], Giacomina Rossi MSc[50], Pietro Tiraboschi MD[50], Diana Duro NPsych[51], Maria Rosario Almeida PhD[51], Miguel Castelo-Branco MD PhD[51], Maria João Leitão BSc[52], Miguel Tabuas-Pereira MD[53], Beatriz Santiago MD[53], Serge Gauthier MD[56], Pedro Rosa-Neto MD PhD[57], Michele Veldsman PhD[58], Toby Flanagan BSc[60], Catharina Prix MD[61], Tobias Hoegen MD[61], Elisabeth Wlasich Mag. rer. nat.[61], Sandra Loosli MD[61], Sonja Schonecker MD[61], Elisa Semler Dr.hum.biol Dipl. Psych[62], Sarah Anderl-Straub Dr.hum.biol Dipl.Psych[62], Luisa Benussi PhD[63], Giuliano Binetti MD[63], Michela Pievani PhD[63], Gemma Lombardi MD[64], Benedetta Nacmias PhD[64], Camilla Ferrari[64], Valentina Bessi[64], Cristina Polito[65].

Affiliations

[1]Dementia Research Centre, Department of Neurodegenerative Disease, UCL Queen Square Institute of Neurology, London, UK; [2]Dementia Research Institute, Department of Neurodegenerative Disease, UCL Institute of Neurology, Queen Square, London, UK; [3]Center for Neurodegenerative Science, Van Andel Research Institute, Grand Rapids, Michigan, USA.[4]Department of Medical Statistics, London School of Hygiene and Tropical Medicine, London, UK; [5]MRC Prion Unit, Department of Neurodegenerative Disease, UCL Institute of Neurology, Queen Square, London, UK; [6]Department of Neurology, Erasmus Medical Centre, Rotterdam, Netherlands; [7]Department of Clinical Genetics, Erasmus Medical Centre, Rotterdam, Netherlands; [8]Amsterdam University Medical Centre, Amsterdam VUmc, Amsterdam, Netherlands; [9]Cognitive Disorders Unit, Department of Neurology, Donostia University Hospital, San Sebastian, Gipuzkoa, Spain; [10]Neuroscience Area, Biodonostia Health Research Institute, San Sebastian, Gipuzkoa, Spain; [11]OSATEK, University of Donostia, San Sebastian, Gipuzkoa, Spain; [12]CITA Alzheimer, San Sebastian, Gipuzkoa, Spain; [13]Alzheimer's disease and Other Cognitive Disorders Unit, Neurology Service, Hospital Clínic, Barcelona, Spain; [14]Imaging Diagnostic Center, Hospital Clínic, Barcelona, Spain; [15]Centre for Neurodegenerative Disorders, Neurology Unit, Department of Clinical and Experimental Sciences, University of Brescia, Brescia, Italy; [16]Neuroradiology Unit, University of Brescia, Brescia, Italy; [17]Biotechnology Laboratory, Department of Diagnostics, Spedali Civili Hospital, Brescia, Italy; [18]Clinique Interdisciplinaire de Mémoire Département des Sciences Neurologiques Université Laval Québec, Quebec, Canada; [19]Sunnybrook Health Sciences Centre, Sunnybrook Research Institute, University of Toronto, Toronto, Canada; [20]Tanz Centre for Research in Neurodegenerative Diseases, University of Toronto, Toronto, Canada; [21]Baycrest Health Sciences, Rotman Research Institute, University of Toronto, Toronto, Canada; [22]The University Health Network, Toronto Rehabilitation Institute, Toronto, Canada; [23]The University Health Network, Krembil Research Institute, Toronto, Canada; [24]Department of Geriatric Medicine, Karolinska University Hospital-Huddinge, Stockholm, Sweden; [25]Department of Clinical Neuroscience, Karolinska Institutet, Stockholm, Sweden; [26]Division of Clinical Geriatrics, Karolinska Institutet, Stockholm, Sweden; [27]Center for Alzheimer Research, Divison of Neurogeriatrics, Karolinska Institutet, Stockholm, Sweden; [28]Fondazione IRCCS Ca' Granda Ospedale Maggiore Policlinico, Neurodegenerative Diseases Unit, Milan, Italy; [29]University of Milan, Centro Dino Ferrari, Milan, Italy; [30]Department of Neurosciences, Psychology, Drug

Research and Child Health (NEUROFARBA), University of Florence, Florence, Italy; [31]Department of Clinical Neurosciences, University of Cambridge, Cambridge, UK; [32]Department of Clinical Neurological Sciences, University of Western Ontario, London, Ontario Canada; [33]Department of Medical Biophysics, The University of Western Ontario, London, Ontario, Canada; [34]Centre for Functional and Metabolic Mapping, Robarts Research Institute, The University of Western Ontario, London, Ontario, Canada; [35]Department of Neuroscience, Mayo Clinic, Jacksonville, Florida, USA; [36]Department of Neurodegenerative Diseases, Hertie-Institute for Clinical Brain Research and Center of Neurology, University of Tübingen, Tübingen, Germany; [37]Center for Neurodegenerative Diseases (DZNE), Tübingen, Germany; [38]Division of Neuropsychology, Hertie-Institute for Clinical Brain Research and Center of Neurology, University of Tübingen, Tübingen, Germany; [39]Department of Diagnostic and Interventional Neuroradiology, University of Tübingen, Tübingen, Germany; [40]Laboratory for Cognitive Neurology, Department of Neurosciences, KU Leuven, Leuven, Belgium; [41]Neurology Service, University Hospitals Leuven, Belgium, Laboratory for Neurobiology, VIB-KU Leuven Centre for Brain Research, Leuven, Belgium; [42]Geriatric Psychiatry Service, University Hospitals Leuven, Belgium; [43]Neuropsychiatry, Department of Neurosciences, KU Leuven, Leuven, Belgium; [44]Laboratory of Neurosciences, Institute of Molecular Medicine, Faculty of Medicine, University of Lisbon, Lisbon, Portugal; [45]Faculty of Medicine, University of Lisbon, Lisbon, Portugal; [46]Laboratory of Language Research, Centro de Estudos Egas Moniz, Faculty of Medicine, University of Lisbon, Lisbon, Portugal; [47]Department of Neurosciences and Mental Health, Centro Hospitalar Lisboa Norte - Hospital de Santa Maria & Faculty of Medicine, University of Lisbon, Lisbon, Portugal; [48]Instituto Ciencias Nucleares Aplicadas a Saude, Universidade de Coimbra, Coimbra, Portugal; [49]Neuropathology Unit and Department of Neurology, Centro Hospitalar do Porto - Hospital de Santo António, Oporto, Portugal; [50]Fondazione IRCCS Istituto Neurologico Carlo Besta, Milano, Italy; [51]Faculty of Medicine, University of Coimbra, Coimbra, Portugal; [52]Centre of Neurosciences and Cell biology, Universidade de Coimbra, Coimbra, Portugal; [53]Neurology Department, Centro Hospitalar e Universitario de Coimbra, Coimbra, Portugal; [54]Department of Psychiatry, McGill University Health Centre, McGill University, Montreal, Québec, Canada; [55]McConnell Brain Imaging Centre, Montreal Neurological Institute, McGill University, Montreal, Québec, Canada; [56]Alzheimer Disease Research Unit, McGill Centre for Studies in Aging, Department of Neurology & Neurosurgery, McGill University, Montreal, Québec, Canada; [57]Translational Neuroimaging Laboratory, McGill Centre for Studies in Aging, McGill University, Montreal, Québec, Canada; [58]Nuffield

Department of Clinical Neurosciences, Medical Sciences Division, University of Oxford, Oxford, UK; [59]Faculty of Medical and Human Sciences, Institute of Brain, Behaviour and Mental Health, University of Manchester, Manchester, UK; [60]Faculty of Biology, Medicine and Health, Division of Neuroscience and Experimental Psychology, University of Manchester, Manchester, UK; [61]Neurologische Klinik, Ludwig-Maximilians-Universität München, Munich, Germany; [62]Department of Neurology, University of Ulm, Ulm; [63]Instituto di Ricovero e Cura a Carattere Scientifico Istituto Centro San Giovanni di Dio Fatebenefratelli, Brescia, Italy; [64]Department of Neuroscience, Psychology, Drug Research, and Child Health, University of Florence, Florence, Italy. [65]Department of Biomedical, Experimental and Clinical Sciences “Mario Serio”, Nuclear Medicine Unit, University of Florence, Florence, Italy.